Long-Distance Swirl Gravity from Chiral Swirling Knots with Central Holes

Omar Iskandarani*

September 30, 2025

Abstract

In Swirl–String Theory (SST), long-range attraction arises from the topology of *chiral swirling knots*—vortex filaments including the trefoil (3_1), cinquefoil (5_1), 5_2, and stevedore (6_1). Each knot surrounds a straight rotation axis that carries the circulation. By Cauchy's integral theorem [1, 2], loops that link this axis exhibit an integer plateau of circulation, which we record with the Swirl Clock $S^{\circlearrowleft}_{(t)}$. When two composite tubes (e.g., the proton cores in H_2) share a central axis across an equal-pressure boundary, additive circulation deepens the common pressure well, consistent with attraction between neutral molecules in flat space [3, 4]. A crisp laboratory discriminator follows from the swirl–EM correspondence: topology changes in the swirl network generate geometry-independent, discrete electromotive impulses of fixed magnitude, $\Delta\Phi = \pm\Phi_\star$ [5, 6], with sign set by chirality. Non-integral steps, geometry-dependent amplitudes, or persistence without verified linking would falsify this mechanism.

1 Chiral Swirling Knots and Central Holes

Consider a chiral knot K embedded in $\mathbb{R}^3$, such as Fig. 1:

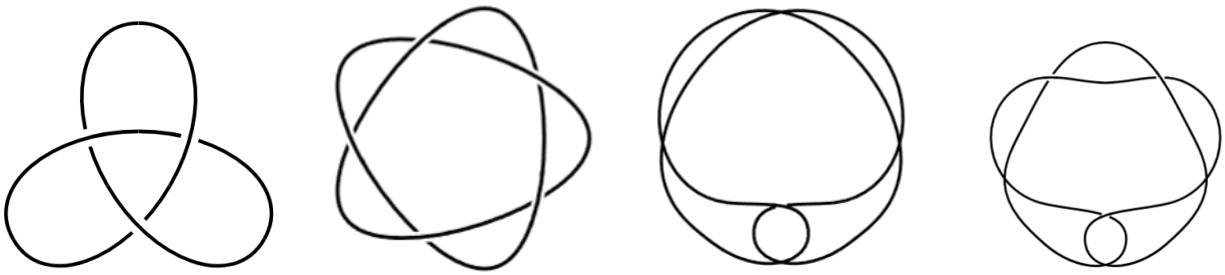

(a) 3_1 (trefoil) (b) 5_1 (cinquefoil) (c) 5_2 (cinquefoil twist) (d) 6_1 (stevedore)

Figure 1: Canonical knot gallery.

Each knot can be parametrized on a torus with major radius R and minor radius r. The core tube of radius r_c supports a tangential swirl velocity $\mathbf{v}_{\circlearrowleft}$, defining the *Swirl Clock* $S^{\circlearrowleft}_{(t)}$.
A key structural feature is a *central hole* threaded by a straight axis (taken as the z-axis), along which the analytic swirl potential is singular.

* Independent Researcher, Groningen, The Netherlands
Email: info@omariskandarani.com
ORCID: 0009-0006-1686-3961
DOI: 10.5281/zenodo.17204124
Keywords: Swirl-String Theory, Topological Gravity, Entropic Force, Circulation Quantization, Flat-Space Field Theory

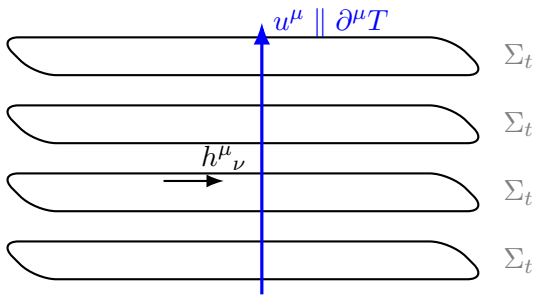

Figure 2: Preferred foliation by the clock field $T(x)$ with unit timelike u^μ, and spatial projector $h_{\mu\nu} = g_{\mu\nu} + u_\mu u_\nu$.

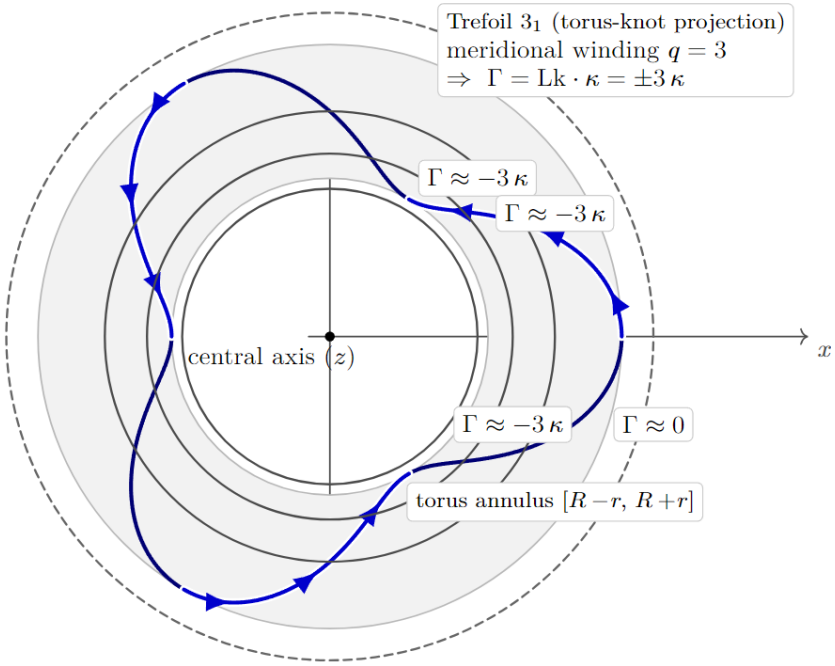

Figure 3: Trefoil knot with central axis and circulation loops in the z=0 plane. Loops whose spanning disk intersects the filament within the torus annulus measure a plateau $\Gamma = \mathrm{Lk} \cdot \kappa = \pm 3\,\kappa$ (sign by orientation). Loops outside the annulus do not enclose the filament and give $\Gamma \approx 0$.

2 Cauchy Integral and Circulation Quantization

Let C be a closed loop in the x–y plane encircling the z-axis. For an analytic swirl potential $W(z) = \Phi + i\Psi$ in a simply connected region,

$$\oint_C \mathbf{v}_\circlearrowleft \cdot d\mathbf{l} = \begin{cases} 0, & \text{if no singularity inside,} \\ 2\pi i \,\mathrm{Res}\left(\frac{dW}{dz}, z = 0\right), & \text{if the axis is enclosed.} \end{cases} \tag{1}$$

In SST we identify the residue with a circulation quantum κ. Independently of the complex-potential language, Kelvin's theorem fixes circulation [7, 8, 9, 10] on any material loop; both viewpoints agree on the integer plateau:

$$\Gamma_C = n\,\kappa \quad \text{if the loop links } n \text{ times with the core.} \tag{2}$$

Canonical identification of κ (SST)

We adopt the equivalence

$$\boxed{\kappa \equiv \frac{h}{m_{\text{eff}}} \;=\; 2\pi\, r_c\, v_c}$$

which gives a direct bridge between the quantum of circulation and core kinematics. Hence

$$m_{\text{eff}} \;=\; \frac{h}{2\pi r_c v_c}\,.$$

Numerics (SI): with $r_c = 1.408\,970\,17 \times 10^{-15}\,\text{m}$ and $v_c = \|\mathbf{v}_{\circlearrowleft}\| = 1.093\,845\,63 \times 10^{6}\,\text{m/s}$,

$$\kappa = 2\pi r_c v_c = 9.683\,619\,2 \times 10^{-9}\,\text{m}^2/\text{s}, \qquad m_{\text{eff}} = \frac{h}{\kappa} = 6.842\,555 \times 10^{-26}\,\text{kg} \approx 38.384\,\text{GeV/c}^2.$$

Status/limits: Dimensions are consistent ($[\kappa] = L^2T^{-1}$). For loops whose spanning disk intersects the torus annulus of the filament, Γ plateaus at $n\kappa$; for loops entirely outside, $\Gamma \approx 0$ (as illustrated in Fig. 3).

Swirl–EM correspondence (operational note)

In the Canon's swirl–EM mapping, time-varying core areal density acts as a "source" via a term of the form $b^{\circlearrowleft} = G^{\circlearrowleft}\,\partial_t \varrho^{\circlearrowleft}$, providing a handle for experimental couplings. Dynamics on the central line that modulate $\varrho^{\circlearrowleft}$ can therefore seed measurable EM-like responses without curving space, consistent with the flat-space treatment used here.

3 Composite Baryon Tubes

Inside baryons, three quark knots (e.g., 5_2, 5_2, 6_1; see Figs. 1c and 1d) meet at a Y-shaped junction, forming a single composite swirl tube (Fig. 4).

Each quark knot i has circulation $\Gamma_i = \kappa$ around the central axis (Fig. 4c). By Kelvin's theorem (linearity of circulation),

$$\Gamma_{\text{baryon}} = \Gamma_1 + \Gamma_2 + \Gamma_3 = 3\kappa. \tag{3}$$

Since $\Gamma = 2\pi r\, v_\theta$,

$$\boxed{v_{\theta,\text{eff}} = \frac{\Gamma_{\text{baryon}}}{2\pi\, r_{\text{eff}}} = \frac{3\kappa}{2\pi\, r_{\text{eff}}}\,,} \tag{4}$$

with r_{eff} the effective core radius of the merged tube. In the thin-core, near-Rankine limit $r_{\text{eff}} \approx r_c$ to leading order (so that $v_{\theta,\text{eff}} \approx 3v_c$ holds as a first-order estimate), while the deeper pressure well is set by the increased Γ.

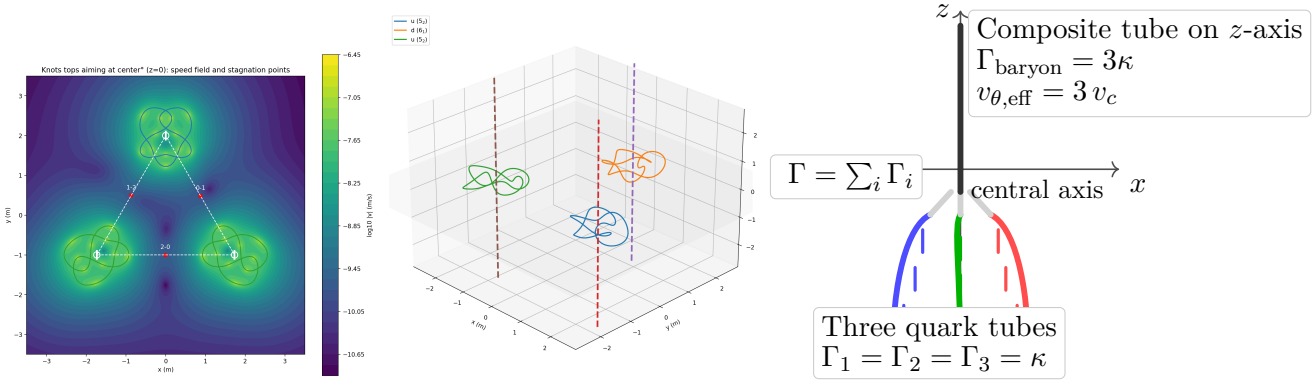

(a) Top view of 3 quark knots (b) 3D view of 3 quark knots (c) Composite tube

Figure 4: Baryon core as a *composite swirl tube*. Three quark tubes (bottom) join via a Y-junction into a single tube along $+z$. Circulation adds linearly, $\Gamma_{\text{baryon}} = 3\kappa$, hence $v_\theta, \text{eff} = \Gamma_{\text{baryon}}/(2\pi r_{\text{eff}})$ with $r_{\text{eff}} \approx r_c$ to leading order.

Swirl Clock scaling. The Swirl Clock relation becomes

$$dt_{\text{local}} = dt_\infty \sqrt{1 - \frac{(3v_c)^2}{c^2}}, \tag{5}$$

predicting a more pronounced local time dilation, consistent with the larger rest mass of baryons relative to single quark knots.

Analogy (for intuition). Three equal water whirls feed one outlet: the hole may widen slightly, but the combined spin deepens the whirl and speeds the rim roughly threefold.

4 Swirl Gravity and Molecular Attraction

Two composite tubes (e.g., two protons) that share the same central line produce a combined circulation

$$\Gamma_{\text{total}} = (3\kappa)_{\text{proton}} + (3\kappa)_{\text{proton}} = 6\kappa,$$

which deepens the shared pressure well and yields a stronger long-range attraction. This is consistent with the observation that neutral molecules (e.g., H_2) attract in Euclidean space [3, 4]: their baryon cores can be connected by the same central line, with the resulting swirl contribution following from additive circulation.

4.1 Electromotive Response to Swirl Gravity

Recent work in the SST Canon [11] indicates that time-dependent swirl density $\partial_t \vec{\rho}_{\circlearrowleft}$ acts as a source term in a modified Faraday law:

$$\nabla \times \vec{E} = -\partial_t \vec{B} - \vec{b}_{\circlearrowleft}, \quad \vec{b}_{\circlearrowleft} = G_{\circlearrowleft}\, \partial_t \vec{\rho}_{\circlearrowleft}$$

Here, $G_{\circlearrowleft}$ is a universal topological transduction constant, canonically normalized to a flux quantum $\Phi^\star \in \{h/e, h/2e\}$. For the formal derivation, see Appendix A. This coupling leads to a falsifiable prediction: nucleation or reconnection of vortex lines produces a quantized electromotive impulse of magnitude $\Phi^\star$. In gravitational contexts, pressure or density changes that alter swirl topology should

have electromagnetic correlates. Thus, SST gravity is fluid-mechanical and electromagnetically active—features that can be tested in vortex-generating platforms.

Companion Paper Reference

The modified Faraday law [11] with the swirl–induced source term (4.1) is derived in a companion manuscript [11]. There, it is shown that $G_{\circlearrowleft}$ is quantized in Weber units and identified with a flux quantum [5, 6], $G_{\circlearrowleft} = \Phi_\star \in \{h/e,\, h/2e\}$. In the present work we focus on experimental implications.

5 Experimental Realization of Swirl-Induced Electromotive Impulses

5.1 Prediction

Topological transitions in the swirl sector (nucleation, annihilation, reconnection of swirl lines) generate quantized electromotive impulses,

$$\Delta\Phi = \pm\,\Phi_\star, \qquad \Phi_\star \in \left\{\tfrac{h}{e},\, \tfrac{h}{2e}\right\}, \tag{6}$$

observable in any linked detection loop, independent of loop geometry. The sign of the impulse is set by chirality.

5.2 Condensed-Matter Implementation

Viable condensed-matter testbeds include:

- Type-II superconducting thin films with vortex entry/exit control,
- Quasi-2D atomic Bose–Einstein condensates,
- Magnetic skyrmion or Hopfion films.

A lithographed multi-turn superconducting micro-coil is positioned such that the defect line threads the loop during a topological transition. The induced impulse voltage is

$$V_{\text{imp}} \approx \frac{N\,\Phi_\star}{\Delta t}, \tag{7}$$

where N is the number of turns and Δt is the event timescale.

Numerical example. For $N = 1000$, $\Phi_\star = h/2e \approx 2.07 \times 10^{-15}\,\text{Wb}$, and $\Delta t = 10\,\text{ns}$,

$$V_{\text{imp}} \approx 0.207\,\text{mV}.$$

For $\Delta t = 1\,\text{ns}$, $V_{\text{imp}} \approx 2.07\,\text{mV}$.

5.3 Protocol and Statistics

1. Prepare the platform under controlled (T, B, P).
2. Trigger a single topological transition.
3. Record the transient voltage.

4. Repeat for 10^3–10^5 events.

5. Histogram the normalized flux $\int V(t)\,dt/N$.

Expected result: discrete peaks at integer multiples of $\Phi_\star$, sign-flip under chirality reversal, invariance under linking-preserving deformations, collapse under unlinking or resistive replacement.

5.4 Hydrogenic and Atomic Systems

Swirl-Clock modulation predicts small line shifts in hydrogen, H^-, and H_2. High-resolution spectroscopy can be complemented with a micro-coil near the sample to detect coincident quantized impulses during internal topological transitions.

5.5 Falsifiability Criteria

- Quantization: impulses in steps of $\Phi_\star$,
- Chirality: reversal flips sign,
- Linking number protection: preserved under deformations, destroyed by unlinking,
- Geometry independence: magnitude depends only on N and Δt.

6 Galactic Rotation and Dark Matter Analogue

In addition to the molecular-scale picture, applying the same circulation quantization at galactic scales yields a two-component rotation profile that can reproduce flattened curves without introducing a separate non-baryonic halo *within this model*. Let the azimuthal swirl velocity decompose into a core and a tail contribution:

$$v_\phi(r) \;=\; v_{\text{core}}(r) \;+\; C_{\text{tail}}\left(1 - e^{-r/r_c}\right), \tag{8}$$

where $v_{\text{core}}(r)$ arises from finite baryonic-core circulation and the second term represents saturation of swirl transmission into the disk.

Flat rotation curves. In the limit $r \gg r_c$, Eq. (8) asymptotes to

$$v_\phi(r) \;\longrightarrow\; C_{\text{tail}},$$

producing flattened rotation curves. This is a hydrodynamic consequence of circulation quantization and saturation in the present framework.

Finite energy density. The swirl energy density associated with the tail is

$$\rho_E(r) \;=\; \tfrac{1}{2}\,\rho_f\,v_\phi^2(r) \;\longrightarrow\; \tfrac{1}{2}\,\rho_f\,C_{\text{tail}}^2 \quad (r \to \infty), \tag{9}$$

which remains finite. Thus the apparent "dark halo" corresponds, in this model, to a constant swirl–energy plateau rather than an infinite mass distribution.

Chirality selection. Following the chiral–achiral selection principle developed in earlier VAM work, only *chiral* knots couple coherently to the galactic swirl clock $S_t^{\circlearrowleft}$. Achiral excitations (Fig. 5) fail to bind and are repelled from high–vorticity regions, precluding virialized halos.

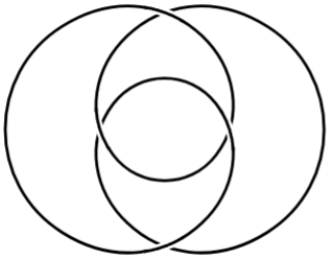

Figure 5: An achiral 4_1 configuration (illustrative).

Rosetta consistency. Using the Rosetta translation, the constants are fixed as

$$\rho_f \;=\; \frac{\rho_{\text{core}}\, r_c}{\|\mathbf{v}_{\circlearrowleft}\|}\,\Omega, \qquad \rho_E \;=\; \tfrac{1}{2}\,\rho_f\,\|\mathbf{v}_{\circlearrowleft}\|^2, \qquad \rho_m \;=\; \rho_E/c^2,$$

ensuring dimensional consistency across both atomic (hydrogen) and galactic (rotational) scales.

Falsifiers. Two outcomes would challenge the proposal: (i) a system with well-measured baryons and negligible environmental coupling that still requires a full canonical dark-matter halo; (ii) a case where the inferred swirl coupling demands axis linkages that are topologically incompatible with the observed morphology.

Summary. Equation (8) provides a falsifiable, SST-specific analogue of dark-matter phenomenology: flat galactic rotation curves, finite halo energy, and chirality-restricted matter coupling arise from quantized circulation in flat space.

7 Entropic Embedding of Swirl–String Theory

Swirl–String Theory (SST), built on topologically quantized circulation in a flat, vortex-supporting medium, admits an entropic reinterpretation compatible with the core principles of emergent gravity [12, 13, 14, 15, 16], allowing mass, force, and time to be read as information-theoretic quantities.

7.1 Swirl Entropy as Informational Field

We define a swirl-based entropy field $S^{\circlearrowleft}_{(x^\mu)}$ as a logarithmic function of the swirl areal density $\rho_{\circlearrowleft} = \nabla \cdot \vec{a}$:

$$S^{\circlearrowleft}_{(x^\mu)} = k_B \cdot \log\left(1 + \frac{\rho_{\circlearrowleft}(x^\mu)}{\rho_0}\right) \tag{10}$$

Here, ρ_0 is a baseline density. The field $S^{\circlearrowleft}$ plays the role of a local entropy density, similar to that on a holographic screen in entropic gravity.

7.2 Entropic Force from Swirl Gradients

Verlinde's entropic-force expression is:

$$F = T \cdot \frac{dS}{dx} \tag{11}$$

In SST, circulation-induced pressure deficits are

$$\Delta p = -\frac{1}{2}\,\rho_f\, v^2 \tag{12}$$

Assuming that swirl flow aligns with the entropy gradient, the effective force becomes

$$F_{\text{swirl}} \propto \nabla(\rho_f v^2) \propto \nabla S^{\circlearrowleft}, \tag{13}$$

establishing an explicit analogy between entropic forces and swirl-induced attraction in SST.

7.3 Mass as Topological Information

In SST, a mass scale is set by the circulation quantum κ:

$$m = \frac{h}{\kappa}, \qquad \kappa = 2\pi r_c v_c \tag{14}$$

Interpreting κ as a unit of quantized topological information, one may write a discrete sum over informational elements:

$$m_K = \sum_i \epsilon_i, \quad \epsilon_i = \frac{h}{\kappa_i}. \tag{15}$$

7.4 Time Dilation as an Entropic Clock

SST defines a Swirl Clock for local proper time,

$$dt_{\text{local}} = dt_\infty \sqrt{1 - \frac{v^2}{c^2}}, \tag{16}$$

consistent with entropic gravity, where time slows in regions of higher information density, i.e., larger $\rho_{\circlearrowleft}$.

7.5 R/T Phase Transition and Information Localization

SST posits two phases:

- **R-phase**: unknotted, wave-like field state
- **T-phase**: knotted, particle-like topological excitation

The R-to-T transition represents entropic localization, akin to wavefunction collapse and decoherence, aligning SST with entropy-based emergence of space and matter.

7.6 Summary of Mapping

SST may therefore be read as an entropic field theory in flat space, where gravitational and inertial phenomena track topological and informational structures.

SST Concept	Entropic Gravity Analog	Interpretation
$\rho_{\circlearrowleft}$	Entropy density	Local information field
Swirl clock	Gravitational redshift	Entropic time rate
Δp	Entropic force	Gradient of entropy
κ	Info unit / bit	Mass from information
R/T transition	Wave collapse	Information localization

Table 1: Correspondences between SST and Verlinde's entropic gravity.

8 Lagrangian and Action Formulation

The dynamical content of Swirl–String Theory (SST) can be expressed via an effective Lagrangian density $\mathcal{L}$ over flat spacetime, with swirl fields defined by a scalar potential $\phi(x^\mu)$, a swirl vector potential $a_\mu(x^\nu)$, and a fluid mass density field ρ_f. Define the swirl areal density as $\rho_{\circlearrowleft} = \nabla \cdot \vec{a}$. With a Maxwell-like field strength

$$F_{\mu\nu} = \partial_\mu a_\nu - \partial_\nu a_\mu,$$

a representative Lagrangian is

$$\mathcal{L}_{\text{SST}} = -\frac{1}{4} F_{\mu\nu} F^{\mu\nu} + \rho_f \, (\partial_\mu \phi)(\partial^\mu \phi) - V(\phi) + \mathcal{L}_{\text{topo}},$$

where $V(\phi)$ encodes a knot potential and $\mathcal{L}_{\text{topo}}$ collects topological couplings (e.g., braid index, genus).

The action is then $S = \int \mathcal{L}_{\text{SST}} \, d^4x$. Euler–Lagrange equations yield conservation laws and dynamics for both swirl flow and its entropic analogs.

In hydrogenic systems, swirl gradients around knot cores induce pressure deficits that couple to particle motion via Bernoulli–Euler dynamics, reproducing an effective gravitational behavior without spacetime curvature.

> The quantized vortex mass formula, the swirl Schrödinger equation, and finite-core energy regularization were developed in the VAM framework [Iskandarani, 2024]. The present work translates and updates these within SST notation via the Rosetta map [Iskandarani, 2025].

9 Legacy Foundations and Rosetta Translation

The formal structure of Swirl–String Theory (SST) builds on a prior topological-fluid framework, the Vortex–Æther Model (VAM). That model derived physical results from circulation quantization and fluid field dynamics, including a topologically quantized mass formula, a swirl-based Schrödinger equation, and a non-divergent fluid Lagrangian. These are translated within SST via a symbolic mapping documented in the Rosetta file [17, 18].

9.1 Quantized Circulation and Mass Formula

In VAM, a core-mass mechanism arises from Onsager-like circulation quantization [19, 20]:

$$\oint \vec{v} \cdot d\vec{\ell} = n \, \kappa_{\text{æ}} \tag{17}$$

with velocity expressed as a gradient,

$$\vec{v} = \lambda_{æ}\,\nabla\theta, \qquad \psi = \sqrt{\rho/\rho_{æ}}\,e^{i\theta}, \tag{18}$$

leading to a hydrodynamic Schrödinger equation with a swirl potential,

$$i\hbar_{æ}\,\frac{\partial\psi}{\partial t} = -\frac{\hbar_{æ}^2}{2m_{æ}}\,\nabla^2\psi + \Phi_{\text{swirl}}(\vec{\omega})\,\psi, \tag{19}$$

$$\Phi_{\text{swirl}} = \frac{1}{2}\,\lambda_g\,\rho_{æ}\,|\vec{\omega}|^2. \tag{20}$$

Reported vortex-mass estimates (e.g., for the electron) were within $\sim 10^{-7}$ of experimental values in that framework; independent verification is an open task.

9.2 Lagrangian and Field Formalism

VAM provided a fluid Lagrangian consistent with gauge-invariant dynamics:

$$\mathcal{L}_{\text{VAM}} = \frac{1}{2}\,\rho_f\,(\nabla\times\vec{A})^2 + \rho_f\,(\partial_t\phi)^2 - V(\phi). \tag{21}$$

This maps to the SST flat-space field theory as

$$\mathcal{L}_{\text{SST}} = -\frac{1}{4}F_{\mu\nu}F^{\mu\nu} + \rho_f\,(\partial_\mu\phi)(\partial^\mu\phi) - V(\phi) + \mathcal{L}_{\text{topo}}, \tag{22}$$

where the swirl vector a_μ replaces the VAM circulation potential, and $\mathcal{L}_{\text{topo}}$ incorporates topological invariants (braid index, genus, component count).

9.3 Notation Fidelity via Rosetta Map

All constants, fields, and structural equations have been translated via the VAM–SST Rosetta dictionary [18], maintaining dimensional and symbolic consistency. This includes:

- Swirl velocity: $\vec{v}_{\circlearrowleft} = \nabla\phi$
- Core swirl speed: $\|\vec{v}_{\circlearrowleft}\| = 1.093\times10^6$ m/s
- Core radius: $r_c = 1.40897\times10^{-15}$ m
- Core density: $\rho_{\text{core}} = 3.89\times10^{18}$ kg/m^3
- Time variables: external time τ, swirl clock $S(t)$, and proper loop time T_s

This lineage yields a variational, quantized, and empirically calibrated foundation—recast here in a swirl-theoretic, flat-space field formalism.

10 Conclusion

Long-distance attraction in SST is a manifestation of topological quantization: chiral knots with central holes enforce non-vanishing circulation residues along a central line. When multiple quark knots merge into a baryon, their circulations add linearly, forming a single composite tube with 3κ circulation. Two testable consequences follow: (1) discrete electromotive impulses of fixed magnitude $\Delta\Phi = \pm\Phi_\star$ at topology changes; (2) a contribution to large-scale dynamics that flattens rotation curves in systems with axis linkages.

Code and Data Availability

All predictive simulations used in this paper are implemented in the open Python script `SST_INVARIANT_MASS3.py`, available on request or at Zenodo: https://doi.org/10.5281/zenodo.17155854

A Canonical Derivation of the EM–Swirl Coupling (Summary from Canon)

This appendix summarizes the canonical derivation of the EM–swirl coupling as developed in the *Swirl–String Theory Canon* [21]. The goal is to show how time–dependent swirl density enters Maxwell–Faraday dynamics as an additional source term.

Swirl areal density. A coarse–grained swirl density $\rho_{\circlearrowleft}(\mathbf{x}, t)$ is defined as the number of quantized swirl lines per unit area. Its flux through a surface S counts the number of vortex lines piercing S,

$$\Phi_{\circlearrowleft}(t; S) = \int_S \rho_{\circlearrowleft}\, dA = N(S, t) \in \mathbb{Z}.$$

Conservation of circulation (Kelvin invariant) ensures that N is an integer topological quantity that can only change by nucleation, annihilation, or reconnection.[1]

Modified Faraday law. In a rotating–frame foliation, centrifugal and swirl–gravity effects unify into a single effective source $b_{\circlearrowleft}$. The Maxwell–Faraday curl equation becomes

$$\nabla \times \mathbf{E} = -\partial_t \mathbf{B} - \mathbf{b}_{\circlearrowleft}, \qquad \mathbf{b}_{\circlearrowleft} = G_{\circlearrowleft}\, \partial_t \rho_{\circlearrowleft}.$$

Here $G_{\circlearrowleft}$ is a universal transduction constant with dimensions of Weber ($\mathrm{V} \cdot \mathrm{s}$), so that $b_{\circlearrowleft}$ has the same units as $\partial_t B$ ($\mathrm{V} \cdot \mathrm{m}^{-2}$).

Pillbox theorem. Integrating over a surface S and a time interval $[t_i, t_f]$ yields

$$\int_{t_i}^{t_f} \oint_{\partial S} \mathbf{E} \cdot d\ell\, dt = -\Delta\Phi_B(S) - G_{\circlearrowleft}\, \Delta N(S),$$

where $\Delta\Phi_B(S)$ is the magnetic flux change and $\Delta N(S)$ is the net change in vortex number through S. If the magnetic flux is held fixed, the time–integrated EMF reduces to a purely topological impulse proportional to ΔN.

Normalization. The Canon's "electron logic" identifies one topological event ($\Delta N = \pm 1$) with a single flux quantum $\Phi_\star$. This fixes the constant to

$$G_{\circlearrowleft} = \Phi_\star, \qquad \Phi_\star \in \left\{ \tfrac{h}{e},\ \tfrac{h}{2e} \right\},$$

with the choice depending on whether the medium supports single–charge or Cooper–pair transport. This establishes that every topological transition injects a quantized EMF–time impulse, independent of drive details or geometry.

[1] Full derivation available in the supplemental Canon document [21].

Dimensional consistency. Since $[\rho_{\circlearrowleft}] = \mathrm{m}^{-2}$ and $[\partial_t \rho_{\circlearrowleft}] = \mathrm{m}^{-2}\mathrm{s}^{-1}$, multiplying by $[G_{\circlearrowleft}] = \mathrm{V} \cdot \mathrm{s}$ yields $[b_{\circlearrowleft}] = \mathrm{V} \cdot \mathrm{m}^{-2}$, consistent with $[\partial_t B]$.

B Rotating Frame and Flux Quantization

The rotating–frame derivation of the flux impulse is presented in full in the companion paper [11]. The result is that each topological transition generates a quantized time–integrated electromotive force:

$$\int V(t)\, dt = \Phi_\star\, \Delta N, \qquad \Phi_\star \in \left\{ \tfrac{h}{e},\ \tfrac{h}{2e} \right\}.$$

Physical interpretation. This law states that the EMF–time impulse is determined solely by the change in swirl line number (ΔN) and the universal flux quantum $\Phi_\star$. The magnitude is independent of the loop geometry, linking details, or the microscopic rate of the event. Only the sign (set by chirality) and the integer ΔN matter.

Experimental implications. In condensed–matter systems, controlled vortex entry or exit should yield measurable EMF impulses in linked pickup loops. The predicted size is $\sim$0.1–1 mV for $N = 10^3$ turns and nanosecond-scale transitions, well within reach of SQUID or GHz digitizer detection.

Cosmological scaling. At galactic scales, swirl nucleation or reconnection events during mergers should produce transient electromagnetic signatures. Their quantized character provides a falsifiable link between laboratory measurements and astrophysical phenomena.

Falsifiability. Key experimental discriminants are: (i) quantization in units of $\Phi_\star$; (ii) chirality–dependent sign reversal; (iii) invariance under continuous loop deformations that preserve linking number; (iv) collapse of the signal if the loop is unlinked or resistive.

These criteria connect the theoretical derivation of the swirl–EMF coupling directly to measurable laboratory and astrophysical observables.

Summary of Key Points.

- Each topological swirl transition yields an impulse EMF $\Delta\Phi = \pm\Phi_\star$.
- The signal is quantized, chirality-sensitive, and geometry-independent.
- Predictions apply across lab-scale and cosmic scales.

References

[1] Lars V. Ahlfors. *Complex Analysis*. McGraw–Hill, 3rd edition, 1979.

[2] Augustin-Louis Cauchy. Sur les intégrales définies et indéfinies. *Oeuvres complètes*, 1825.

[3] Fritz London. Zur theorie und systematik der molekularkräfte. *Zeitschrift für Physik*, 63:245–279, 1930.

[4] H. B. G. Casimir and Dirk Polder. The influence of retardation on the london–van der waals forces. *Physical Review*, 73(4):360–372, 1948.

[5] B. S. Deaver and W. M. Fairbank. Experimental evidence for quantized flux in superconducting cylinders. *Physical Review Letters*, 7(2):43–46, 1961.

[6] W. A. Little and R. D. Parks. Observation of quantum periodicity in the transition temperature of a superconducting cylinder. *Physical Review Letters*, 9(1):9–12, 1962.

[7] Hermann von Helmholtz. Über integrale der hydrodynamischen gleichungen, welche den wirbelbewegungen entsprechen. *Journal für die reine und angewandte Mathematik*, 1858.

[8] William (Lord Kelvin) Thomson. On vortex motion. *Transactions of the Royal Society of Edinburgh*, 1869.

[9] P. G. Saffman. *Vortex Dynamics*. Cambridge University Press, 1992.

[10] A. J. Majda and A. L. Bertozzi. *Vorticity and Incompressible Flow*. Cambridge University Press, 2002.

[11] Omar Iskandarani. Rotating–frame unification in the sst canon: From swirl density to swirl–emf, and a canonical derivation of the coupling $g_{\circlearrowleft}$. https://doi.org/10.5281/zenodo.17203812, 2025. Version v0.0.1, Sept 25, 2025.

[12] Erik P Verlinde. On the origin of gravity and the laws of newton. *Journal of High Energy Physics*, 2011(4):1–27, 2011.

[13] Erik P Verlinde. Emergent gravity and the dark universe. *SciPost Physics*, 2(3):016, 2017.

[14] Ted Jacobson. Thermodynamics of spacetime: The einstein equation of state. *Physical Review Letters*, 75(7):1260, 1995.

[15] Thanu Padmanabhan. Thermodynamical aspects of gravity: New insights. *Reports on Progress in Physics*, 73(4):046901, 2010.

[16] Jacob D Bekenstein. Black holes and entropy. *Physical Review D*, 7(8):2333, 1973.

[17] Omar Iskandarani. Quantum mechanics and quantum gravity in the vortex Æther model a reformulation using superuid vorticity and topology. https://doi.org/10.5281/zenodo.15870859, 2025. Published via Zenodo and archived at `zenodo.org`.

[18] Omar Iskandarani. Rosetta mapping from vam to swirl–string theory. https://doi.org/10.5281/zenodo.16980377, 2025.

[19] Lars Onsager. Statistical hydrodynamics. *Nuovo Cimento*, 1949.

[20] Richard P. Feynman. Application of quantum mechanics to liquid helium. *Progress in Low Temperature Physics*, 1, 1955.

[21] Omar Iskandarani. Swirl-string theory (sst) canon v0.5.9: Core postulates, constants, and boxed master equations. https://doi.org/10.5281/zenodo.16934535, September 2025. Single source of truth for SST symbols, constants, and canonical equations; required citation for dependent works.